

UC Berkeley

UC Berkeley Previously Published Works

Title

Engineering *Pseudomonas putida* KT2440 for chain length tailored free fatty acid and oleochemical production

Permalink

<https://escholarship.org/uc/item/45n643cj>

Journal

Communications Biology, 5(1)

ISSN

2399-3642

Authors

Valencia, Luis E
Incha, Matthew R
Schmidt, Matthias
et al.

Publication Date

2022

DOI





10.1038/s42003-022-04336-2

Copyright Information

This work is made available under the terms of a Creative Commons Attribution License, available at <https://creativecommons.org/licenses/by/4.0/>

Peer reviewed

Engineering *Pseudomonas putida* KT2440 for chain length tailored free fatty acid and oleochemical production

Luis E. Valencia^{1,2,3}, Matthew R. Incha^{1,2,4}, Matthias Schmidt^{1,2,5}, Allison N. Pearson^{1,2,4}, Mitchell G. Thompson ^{1,6}, Jacob B. Roberts^{1,2,3}, Marina Mehling^{1,2}, Kevin Yin ^{1,2,4}, Ning Sun^{2,7}, Asun Oka^{2,7}, Patrick M. Shih^{1,2,4,6}, Lars M. Blank ⁵, John Gladden^{1,8} & Jay D. Keasling ^{1,2,3,9,10,11}✉

Despite advances in understanding the metabolism of *Pseudomonas putida* KT2440, a promising bacterial host for producing valuable chemicals from plant-derived feedstocks, a strain capable of producing free fatty acid-derived chemicals has not been developed. Guided by functional genomics, we engineered *P. putida* to produce medium- and long-chain free fatty acids (FFAs) to titers of up to 670 mg/L. Additionally, by taking advantage of the varying substrate preferences of paralogous native fatty acyl-CoA ligases, we employed a strategy to control FFA chain length that resulted in a *P. putida* strain specialized in producing medium-chain FFAs. Finally, we demonstrate the production of oleochemicals in these strains by synthesizing medium-chain fatty acid methyl esters, compounds useful as biodiesel blending agents, in various media including sorghum hydrolysate at titers greater than 300 mg/L. This work paves the road to produce high-value oleochemicals and biofuels from cheap feedstocks, such as plant biomass, using this host.

¹Joint BioEnergy Institute, Emeryville, CA 94608, USA. ²Biological Systems and Engineering Division, Lawrence Berkeley National Laboratory, Berkeley, CA 94720, USA. ³Department of Bioengineering, University of California, Berkeley, CA 94720, USA. ⁴Department of Plant and Microbial Biology, University of California, Berkeley, CA 94720, USA. ⁵Institute of Applied Microbiology (iAMB), Aachen Biology and Biotechnology (ABbt), RWTH Aachen University, Aachen, Germany. ⁶Environmental Genomics and Systems Biology Division, Lawrence Berkeley National Laboratory, Berkeley, CA, USA. ⁷Advanced Biofuels and Bioproducts Process Demonstration Unit, Emeryville, CA 94608, USA. ⁸Biomanufacturing and Biomaterials Department, Sandia National Laboratories, Livermore, CA 94550, USA. ⁹Department of Chemical & Biomolecular Engineering, University of California, Berkeley, CA 94720, USA. ¹⁰Center for Biosustainability, Technical University of Denmark, Lyngby, Denmark. ¹¹Center for Synthetic Biochemistry, Institute of Synthetic Biology, Shenzhen Institutes of Advanced Technologies, Shenzhen, China. ✉email: keasling@berkeley.edu

The world has seen a monumental shift to oleochemicals, plant and animal-derived oils and fats, as a substitute for petrochemicals in recent decades^{1,2}. These oleochemicals are a critical renewable feedstock for the industrial production of detergents, lubricants, and biodiesel, among other products³. Palm oil has emerged as the dominant and fastest-growing source of oleochemicals due to its superior productivity of ~4.4 metric tonnes per hectare per year¹. However, there is demand for alternative sources of oleochemicals that rely less on sensitive tropical land use and can provide fatty acids with different physicochemical properties such as shorter chain lengths (<C16), branched chains, and unique stereochemistry^{3,4}. Currently, most biodiesel is derived from plants and results in predominantly long-chain (C16–C18) fatty acid methyl esters (FAMES). These long-chain FAMES have favorable cetane numbers, however, they show poor performance at low temperatures. Consequently, to be used as drop-in fuels, they require blending agents such as short- or branched-chain FAMES^{5,6}. Metabolic engineering of microbes can provide a route to unique oleochemicals that are difficult to obtain from plants & animals, and may have favorable fuel characteristics^{7–10}.

Pseudomonas putida KT2440 is a promising host for industrial oleochemical production due to its remarkable ability to utilize recalcitrant carbon sources found in lignocellulosic biomass^{11,12}, high tolerance to oxidative stress¹², strong redox potential¹³, and favorable growth characteristics¹⁴. Many genetic tools have become available for engineering *P. putida*^{15–17}, and substantial progress has been made in improving its host properties, such as enhanced fitness in bioreactors¹⁸, utilization of plant-derived hydrolysates¹⁹, and tolerance for ionic liquids found in these hydrolysates²⁰. Although *P. putida* has shown itself to be a versatile and robust host for bioproduction^{18,21–23}, to date there has not been a reported strain capable of producing free fatty acids (FFAs), which are important intermediates in oleochemical metabolic pathways as well as valuable precursors for industrial processes²⁴.

To produce FFAs, the host organism must be unable to catabolize FFAs via β -oxidation, and an acyl-ACP thioesterase must

be employed to hydrolyze and offload FFAs from fatty acid biosynthesis^{24,25}. Avoiding β -oxidation of FFAs can be achieved by knocking out fatty acyl-coenzyme A (CoA) ligases responsible for initiating β -oxidation. In contrast to *Escherichia coli*, which only has two CoA ligases involved in β -oxidation²⁶, *P. putida* was recently found to have a much larger repertoire (>4) of CoA ligases involved in FFA degradation. Growth experiments with individual deletion strains of these CoA ligases suggested that they are involved in initiating β -oxidation of FFAs and have different substrate preferences with regard to the carbon chain length of the FFA²⁷.

In this work, we report the development of a *P. putida* strain unable to catabolize medium and long-chain FFAs by knocking out three CoA ligases. This triple knockout strain produced a different profile of FFAs depending on the heterologous thioesterase expressed, achieving a titer of 670 mg/L total FFAs in shake flask culture. A double knockout strain that favors the production of medium-chain FFAs was developed by leveraging the in vivo substrate preferences of the CoA ligases (Fig. 1). This strategy can potentially be employed in other FFA-producing microbes. Finally, a heterologous fatty acid methyltransferase was expressed to generate medium-chain FAMES, achieving a titer of 302 mg/L total FAMES in shake flask cultures.

Results

Engineering *P. putida* to avoid catabolism of medium- and long-chain FFAs. Previously, by using an RB-TnSeq mutant library of *P. putida*, our lab identified several mutants with moderate to severe fitness defects when grown on minimal media containing FFAs as a sole carbon source²⁷. Transposon mutants in CoA ligase genes *PP_0763*, *PP_4549*, and *PP_4550* had particularly strong fitness defects when grown on medium- (C6–C12) and long-chain (C14 \leq) fatty acids. Notably, the strength of the fitness defect varied depending on the mutant and the FFA used. *PP_0763* had a severe fitness defect when grown on C5–C6 FFAs and a moderate defect when grown on C7–C10 FFAs. *PP_4549* had a severe fitness defect when grown on C6–C18 FFAs, and *PP_4550* had a moderate fitness defect when grown on C6–C12

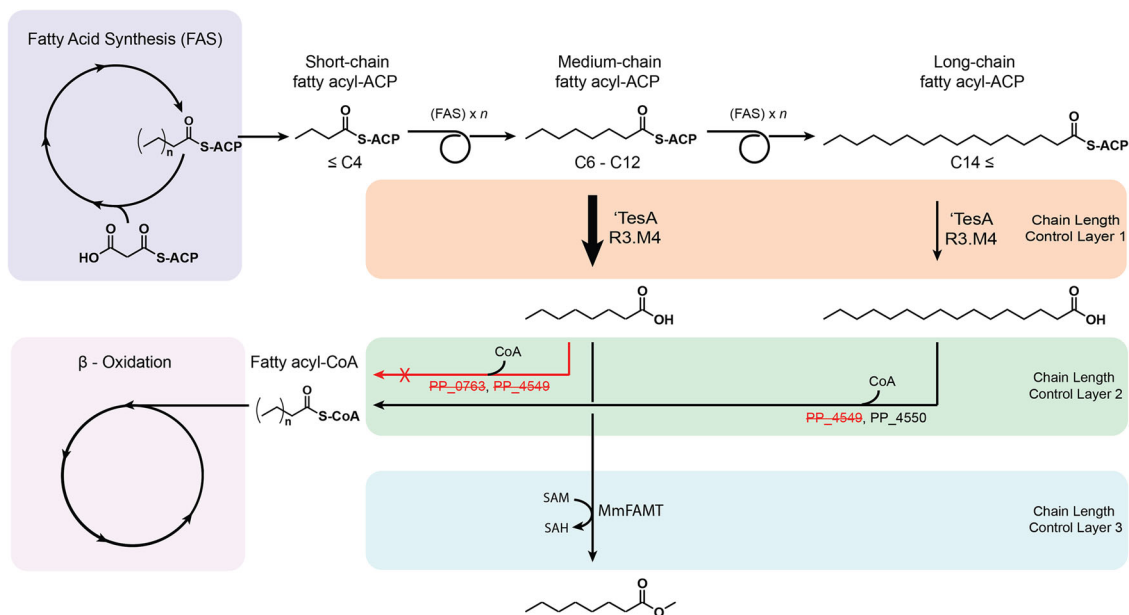


Fig. 1 Multi-layer chain length control strategy. The chain length of the final product is influenced by three layers of control. The use of an engineered acyl-ACP thioesterase favors the production of medium-chain FFAs in layer 1. Selectively knocking out CoA ligases with medium-chain FFA substrate preference prevents the catabolism of medium-chain FFAs while still allowing for catabolism of long-chain FFAs in layer 2. The use of a medium-chain fatty acid methyltransferase further influences the final chain-length profile in layer 3.

FFAs (Supplementary Fig. 1). In this work, we introduced single, double, and triple knockout combinations of these CoA ligase genes and assessed the ability of these mutant strains to catabolize medium- and long-chain FFAs.

We conducted FFA degradation assays with the constructed mutant strains, in which we back diluted overnight cultures into EZ Rich medium containing 10 mM glucose and 250 μ M of each straight-chained FFA with an even-numbered chain length between C6-C16. After a 48-h growth period, FFAs were derivatized & extracted from cultures, quantified via GC/MS, and compared to a media-only control (Fig. 2). Wild-type *P. putida* and single knockouts of ΔPP_{0763} and ΔPP_{4549} were found to degrade more than 80% of each added FFA. The double knockout strains, though still proficient at degrading FFAs, were found to preferentially degrade certain chain lengths depending on which CoA ligases were knocked out. $\Delta PP_{0763} \Delta PP_{4549}$ degraded more than 80% of each FFA except C6, while $\Delta PP_{4549-50}$ degraded more than 80% of each FFA except C14 and C16. This reflects the hypothesis that these CoA ligases have different, yet overlapping, substrate preferences and particular combinations of CoA ligase knockouts may preferentially degrade medium- or long-chain FFAs. The triple knockout strain, $\Delta PP_{0763} \Delta PP_{4549-50}$, hereinafter referred to as 3KO, was found to not degrade any FFAs except C6 and in fact produced small amounts of C8, C12, C14, and C16, likely due to the activity of an endogenous thioesterase. 3KO was able to degrade approximately 30% of the added C6 FFA which may be explained by the activity of *PP_{3553}*, which is predicted to be a short-chain CoA ligase and was reported have a slight fitness defect when grown on hexanoic acid as a sole carbon source²⁷. Finally, 3KO was unable to grow on medium-chain FFAs as a sole carbon source (Supplementary Fig. 2), which further demonstrates that this strain is unable to catabolize medium-chain FFAs via β -oxidation.

Engineering *P. putida* to produce medium- and long-chain FFAs. Following the construction of 3KO, a strain unable to catabolize medium- and long-chain FFAs, we sought to construct strains that actively produce FFAs by overexpressing an acyl-ACP thioesterase. We compiled five engineered variants of ‘TesA, a leaderless version of acyl-ACP thioesterase I from *E. coli*²⁸ (Table 1) and overexpressed each in both wild-type and 3KO background *P. putida* strains via an arabinose-inducible pBADT vector²⁹ (Fig. 3). After a 48-h growth period in either EZ Rich supplemented with 100 mM glycerol or Terrific Broth (TB), FFAs were derivatized and extracted from cultures and quantified via GC/MS. All wild-type background strains produced virtually no FFAs, while all 3KO background strains produced FFAs. All ‘TesA variants produced similar FFA profiles to what was reported in the literature (Table 1) in both EZ Rich and TB media. 3KO containing a pBADT-RFP control plasmid was also found to produce FFAs, primarily C16 and monounsaturated C16 (C16:1), which is likely due to an endogenous thioesterase. Notably, the R3.M4 ‘TesA variant produced the highest titer in both media and produced primarily medium-chain (C6-C12) FFAs. R3.M4 was selected as the ‘TesA variant of choice for future experiments. Interestingly, 3KO strains containing a ‘TesA variant produced isovalerate when grown on TB, perhaps as a degradation product of leucine found in the medium³⁰ (Supplementary Fig. 3).

Given the apparent differences in CoA ligase substrate preference, we hypothesized that expressing R3.M4 in single or double knockout strains would enrich specifically for either medium- or long-chain FFAs because the remaining CoA ligase(s) would still initiate β -oxidation of their preferred FFAs. To achieve this, plasmid 115 was introduced into wild-type, single, double, and triple knockout strains, and FFAs were derivatized and quantified via GC/MS after a 48-h growth period in either EZ Rich supplemented with 100 mM glycerol or TB

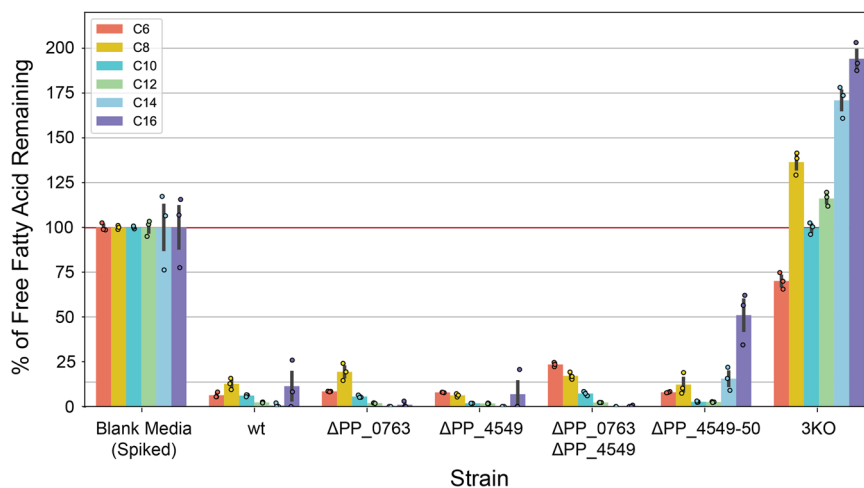


Fig. 2 FFA degradation assays. FFAs concentrations quantified 48 h after strain growth in media spiked with 250 μ M of C6-C16 even-chain FFAs and normalized by FFA concentration in the original spiked media. Values shown represent the mean of biologically independent samples ($n = 3$), and error bars show standard error of the mean.

Table 1 Details of the ‘TesA variants and their pBADT plasmid names used in this study.

‘TesA variant	Plasmid name (this study)	Mutation	Major FFA produced (<i>E. coli</i>)	Ref.
‘TesA	113	N/A	C16	28
L109P	114	L109P	C14, C16	52
R3.M4	115	M141L, Y145K, L146K	C8	40
CM-5	116	E142D, Y145G	C12/C14	53
RD-2	117	M141L, E142D, Y145G, L146K	C8	53

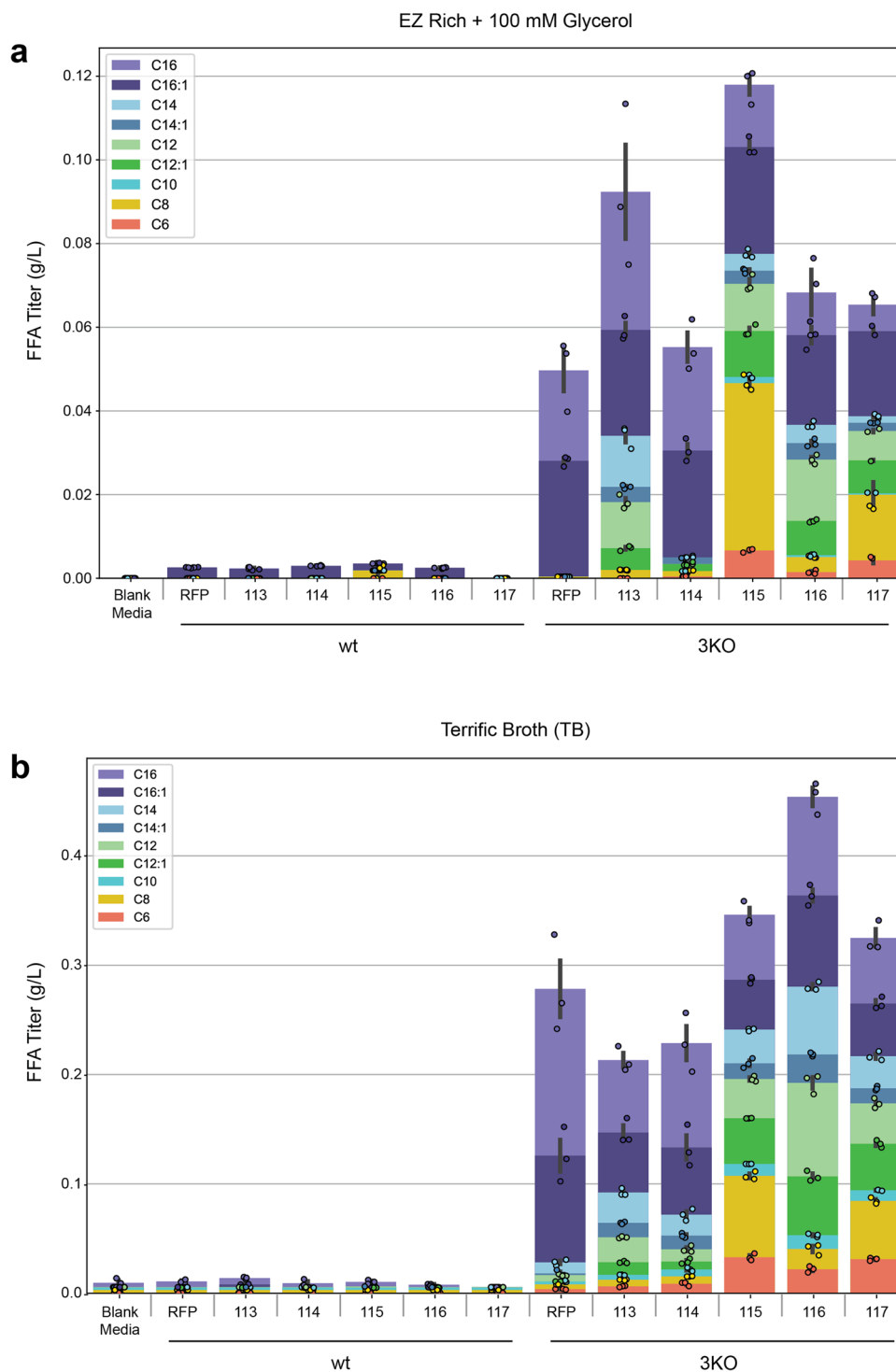


Fig. 3 FFA production profile across various 'Tesa' variants in wt and 3KO background strains. a FFA production in EZ Rich medium supplemented with 100 mM glycerol. **b** FFA production in TB. Values shown represent the mean of biologically independent samples ($n = 3$), and error bars show standard error of the mean.

(Fig. 4). In EZ rich, aside from the 3KO strains which performed similarly to what was reported in Fig. 3, the only strain able to produce a substantial amount of FFAs was $\Delta PP_{0763} \Delta PP_{4549} + 115$, which almost exclusively produced medium-chain FFAs. This result supports the hypothesis that PP_{4550} prefers long-chain FFA substrates; consequently, $\Delta PP_{0763} \Delta PP_{4549}$ is still able to catabolize long-chain FFAs while producing medium-chain FFAs. The same pattern was observed in TB, $\Delta PP_{0763} \Delta PP_{4549} + 115$ almost exclusively produced

medium-chain FFAs. TB is considerably more nutrient rich than EZ Rich, and thus in TB we observed higher titers from all strains, including the double knockout strains $\Delta PP_{0763} \Delta PP_{4549}$ and $\Delta PP_{4549-4550}$ containing the negative control RFP plasmid. FFA production in RFP-containing strains likely results from endogenous thioesterase activity; $\Delta PP_{0763} \Delta PP_{4549} + RFP$ produced mostly medium-chain FFAs while $\Delta PP_{4549-4550} + RFP$ produced long-chain FFAs. The single knockout and double knockout strains containing plasmid 115 also

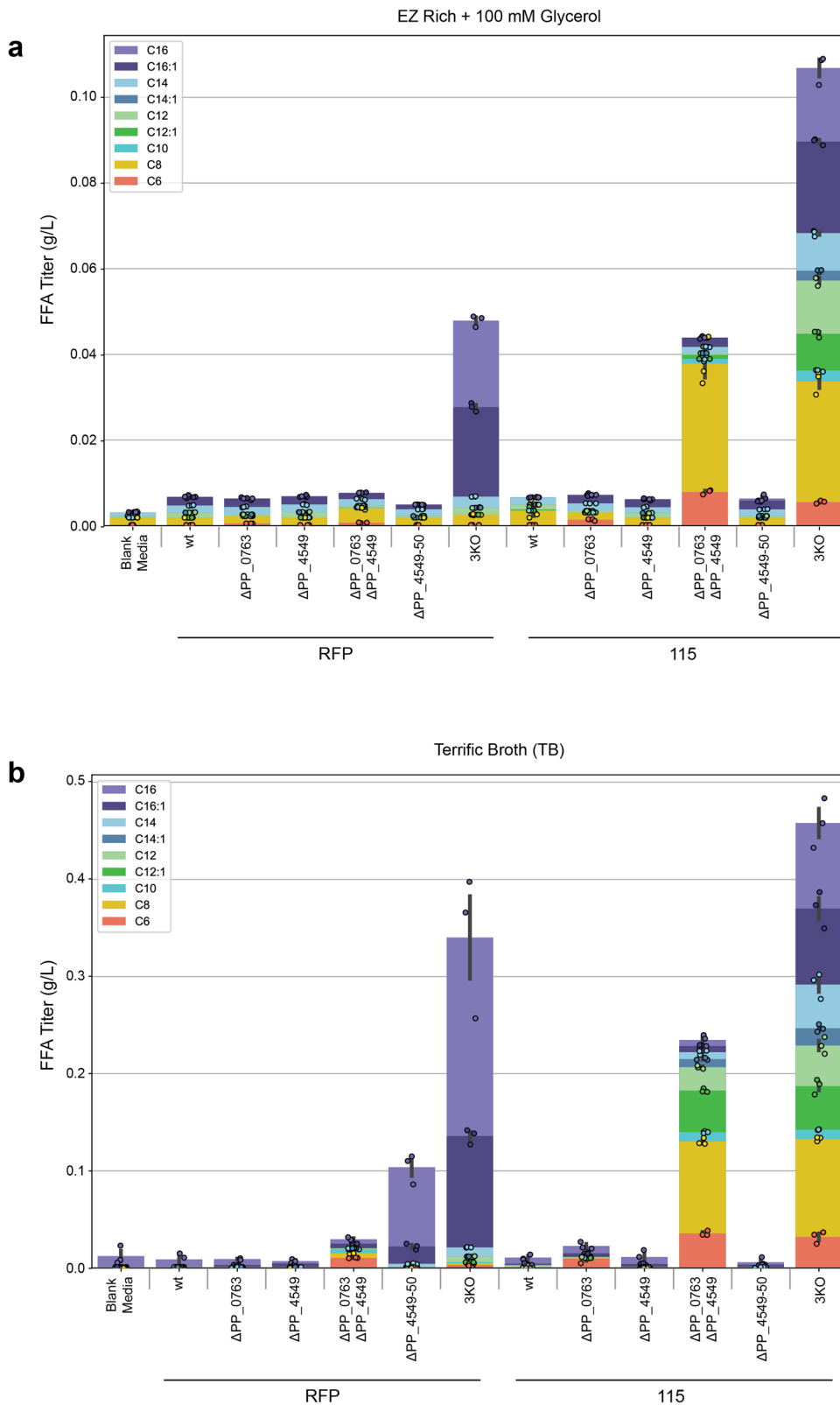


Fig. 4 FFA production profile across various *P. putida* background strains after overexpression of RFP or 'Tesa R3.M4. a FFA production in EZ Rich medium supplemented with 100 mM glycerol. **b** FFA production in TB. Values shown represent the mean of biologically independent samples ($n = 3$), and error bars show standard error of the mean.

produced up to 109.2 mg/L of isovalerate when grown on TB (Supplementary Fig. 3).

Engineering *P. putida* to produce FFA-derived FAMES. To showcase the ability of FFA-producing *P. putida* strains to synthesize FFA-derived oleochemicals, we aimed to produce FAMES by using a fatty acid methyltransferase from *Mycobacterium marinum*, MmFAMT. This methyltransferase works by transferring a methyl group from S-adenosylmethionine (SAM) to a fatty acid carboxyl group and was found to be active on C8, C10, and C12 saturated FFAs and their respective 3-hydroxyacids^{31,32}. MmFAMT was previously used to produce FAMES in *E. coli*, though the highest titers were relatively low, at 16 mg/L, likely because most of the FFAs produced in those *E. coli* strains were long-chain FFAs³². We expected MmFAMT to perform similarly in the *P. putida* knockout strains that favor the production of medium-chain FFAs, the preferred substrate of MmFAMT. To test this, we constructed plasmid 125 from plasmid 115, inserting the engineered *P. putida* RBS JER05³³ and MmFAMT immediately downstream of R3.M4. This plasmid was introduced into the wild-type, single, double, and triple knockout strains. Strains containing plasmid 125 were grown using the same protocol used previously in this study to quantify FFA production. To reduce evaporation of the FAMES, a hydrophobic isopropyl myristate (IPM) overlay was added to each culture. IPM was used as the overlay because it demonstrates low toxicity to *P. putida* (Supplementary Fig. 4), is effective at extracting FAMES, and does not interfere with the chromatography of the FAMES due to its non-overlapping retention time. At the end of the experiment, this overlay was collected and diluted with ethyl acetate containing an internal standard, and FAMES were quantified via GC/MS. To account for partial evaporation, blank media samples with an IPM overlay were spiked with 500 μ M of each medium-chain FAME and incubated alongside FAME-producing cultures. The final measured concentration of FAMES in these spiked blank media samples was used to calculate an evaporation factor that was applied to experimental FAME measurements. The calculated evaporation factor varied depending on the media used, the size of the culture tube or flask, and the chain-length of the FAME (Supplementary Table 1).

In both EZ Rich and TB media, the production of FAMES was observed in all strains containing 125, though the titers varied drastically based on the background strain (Fig. 5). The only FAMES observed were C6, C8, C10, C12:1, and C12, which confirms the medium-chain substrate preference of MmFAMT. All strains grown in EZ Rich produced low titers of FAMES, with the highest titer of 28.1 mg/L being achieved by wild-type + 125. In contrast, when grown in TB, wild-type + 125 was the lowest producing strain whereas the highest producing strains were $\Delta PP_{0763} \Delta PP_{4549}$ and 3KO, with titers of 192.5 mg/L and 163.8 mg/L, respectively. This drastic difference in titers achieved in EZ Rich and TB media is possibly explained by the fact that the methylation step is dependent on the availability of the SAM cofactor, which is produced from methionine and ATP precursors that are more readily available/produced from a very rich medium such as TB. A decreased ability to produce SAM in strains grown in EZ Rich may also explain why the wild-type background strain produced the highest FAMES titer in this medium; the wild-type strain grows comparatively faster than 3KO (Supplementary Fig. 4) and is also able to recycle FFAs as a source of carbon and energy which may help it slightly improve its SAM availability and result in more production of FAMES that are then sequestered into the IPM overlay.

FFA production in strains containing 125 was also measured (Fig. 5). In general, we observed the same FFA production

patterns as in previous experiments, but the effect of CoA ligase substrate preference was amplified for FFAs that could be methylated by MmFAMT. For example, the single knockout $\Delta PP_{0763} + 125$ produced almost exclusively C6, C8, and C12:1 FFA in both media. In contrast $\Delta PP_{0763} + 115$ did not produce appreciable amounts of any FFA. Considering that MmFAMT competes with native CoA ligases for medium-chain FFAs, it is likely that methylation renders a FAME unavailable for CoA ligases. Therefore, in a strain missing a CoA ligase specialized in C6–C12 FFAs, such as ΔPP_{0763} , the MmFAMT is more likely to outcompete the remaining CoA ligases and produce C6–C12 FAMES. In cultures containing an overlay, these FAMES are sequestered into the overlay. In cultures without an overlay, the majority of the FAMES evaporate, otherwise they remain in solution or hydrolyze (either spontaneously or by the action of a methyl ester esterase such as *bioH*)³⁴. FAMES that remain in solution or are hydrolyzed will both result in an elevated FFA measurement. Similarly, $\Delta PP_{4549} + 125$ produced primarily C12:1 and C12 FFAs, while $\Delta PP_{4549} + 115$ did not produce appreciable amounts of FFAs. $\Delta PP_{0763} \Delta PP_{4549} + 125$ produced exclusively medium-chain FFAs with a particular abundance of C8. This finding is expected since the sample's background strain cannot catabolize medium-chain FFAs, possesses a thioesterase specialized in making medium-chain FFAs, and contains a methyltransferase with a medium-chain FFA substrate preference.

Shake flask production runs and media comparisons. To further assess the potential for *P. putida* to produce FFAs and FFA-derived oleochemicals, we conducted production runs of select strains using EZ Rich + 100 mM glycerol, TB, and 4x diluted sorghum hydrolysate. Sorghum hydrolysate is a rich medium derived from plant lignocellulosic biomass and is attractive due to its industrial relevance as a carbon-neutral and plant-derived feedstock for the production of biofuels and bioproducts³⁵. Following dilution, the hydrolysate contained 11.8 g/L glucose, 6.4 g/L xylose, 4.2 g/L acetic acid, 4.3 g/L lactic acid, and unquantified amounts of choline and lignin monomers which *P. putida* can use as sources of carbon and energy³⁶. Due to the high sugar and ionic liquid content of sorghum hydrolysate, strains were gradually adapted to grow in diluted media (see methods). Since fatty acid biosynthesis is an energy and redox-intensive process¹³, these production runs were conducted at a volume of 12.5 mL in 250-mL unbaffled shake flasks to provide optimal aeration. Growth in unbaffled flasks increased titers relative to 5 mL culture tubes across all samples; results are summarized in Fig. 6 and Supplementary Tables 2 and 3. Additionally, yield calculations were conducted for strains grown in EZ Rich + 100 mM glycerol and are summarized in Supplementary Tables 4–7.

Notably, C8 FFA and C8 FAME were the major products in all strains containing 115 and 125, respectively. This reflects the FFA profile produced by the R3.M4 thioesterase. Additionally, $\Delta PP_{0763} \Delta PP_{4549}$ strains were enriched in medium-chain FFAs compared to 3KO strains, which had a more even distribution of medium- and long-chain FFAs. Interestingly, although FAME production improved across all experiments in shake flasks, it did not have a clear correlation with FFA titers. This suggests that although it is important to have a supply of medium-chain FFAs for MmFAMT to utilize, cryptic regulatory or metabolic flux influences might also affect final titers. The highest total FFA titer achieved was 670.9 mg/L, produced by 3KO + 115 in TB. The highest C8 FFA titer, 253.6 mg/L, was observed when $\Delta PP_{0763} \Delta PP_{4549} + 115$ was grown in TB. The greatest FAME titer was also achieved in TB; $\Delta PP_{0763} \Delta PP_{4549} + 125$ in TB produced 302.4 mg/L total FAMES.

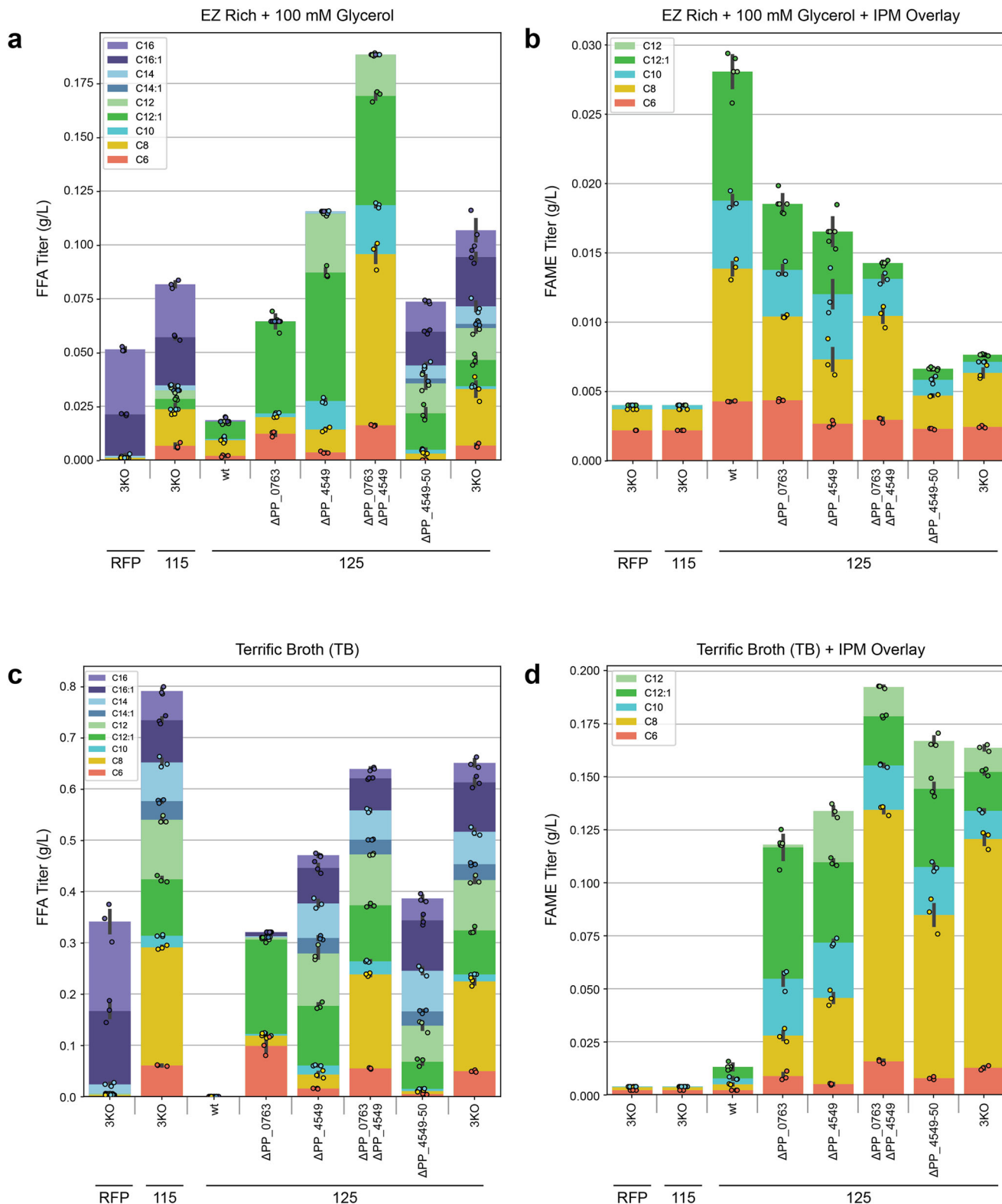


Fig. 5 FFA and FAME production profile across various *P. putida* background strains after overexpression of RFP, 'TesA R3.M4 only, or 'TesA R3.M4 & MmFAMT. a FFA production in EZ Rich medium supplemented with 100 mM glycerol. **b** FAME production in EZ Rich media supplemented with 100 mM glycerol. **c** FFA production in TB. **d** FAME production in TB. Values shown represent the mean of biologically independent samples ($n = 3$), and error bars show standard error of the mean.

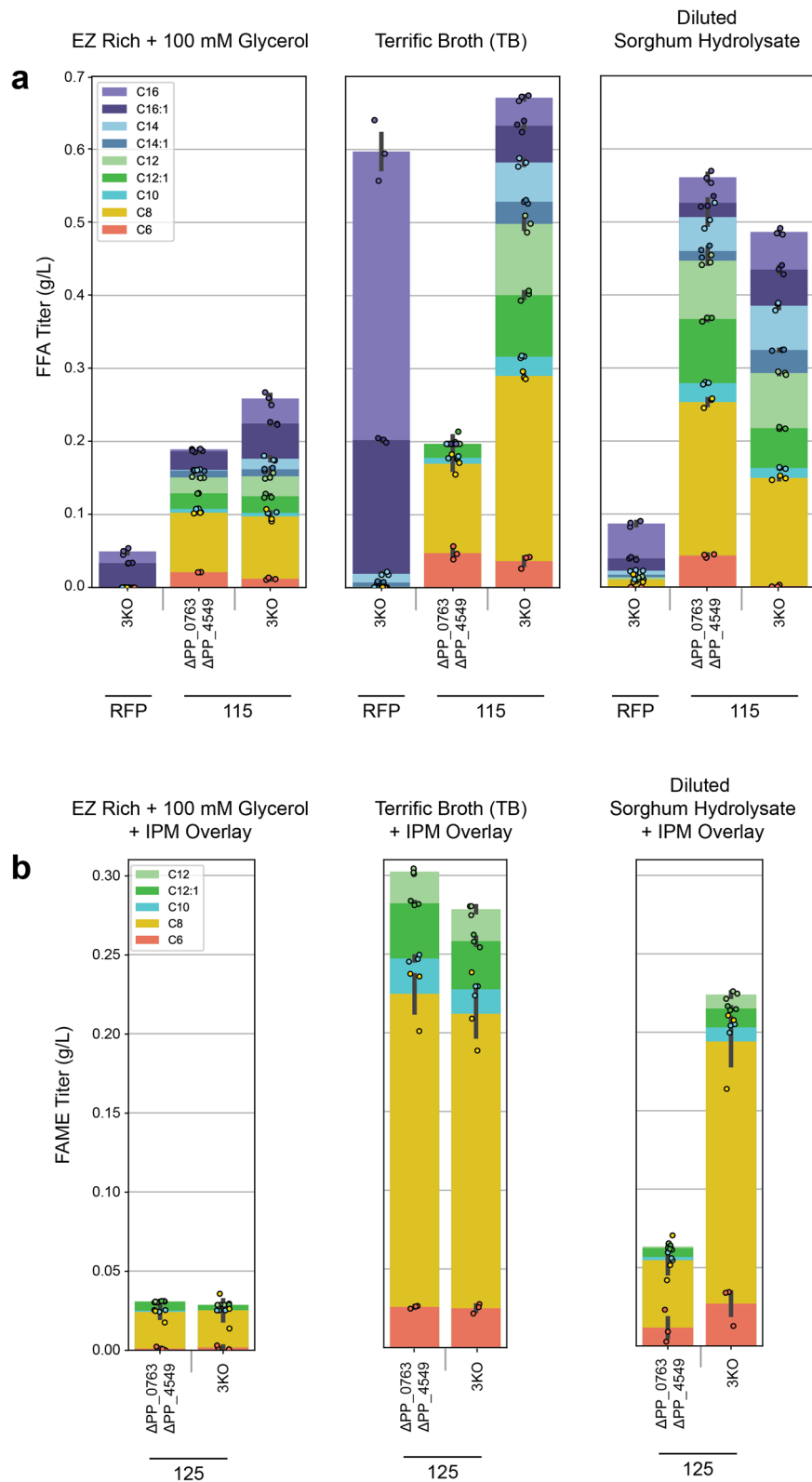


Fig. 6 FFA and FAME production profile in various *P. putida* strains after growth in 250 mL shake flask cultures. a FFA production in EZ Rich medium supplemented with 100 mM glycerol, TB, and diluted sorghum hydrolysate. **b** FAME production in EZ Rich medium supplemented with 100 mM glycerol, TB, and diluted sorghum hydrolysate. Values shown represent the mean of biologically independent samples ($n = 3$), and error bars show standard error of the mean.

Additionally, FFA and FAME titers from strains grown in diluted sorghum hydrolysate approached levels achieved in TB. In diluted sorghum hydrolysate, $\Delta PP_{0763} \Delta PP_{4549} + 115$ produced 561.1 mg/L total FFAs, the majority of which were medium-chain FFAs, while 3KO + 125 produced 224.0 mg/L total FAMES. This further demonstrates the potential for using *P. putida* to sustainably produce oleochemicals from plant-derived carbon sources.

Discussion

There has been a notable shift to plant and animal-derived oleochemicals as a substitute for petrochemicals. Microbial oleochemical production offers a versatile additional source of oleochemicals with unique properties such as branched-chains or shorter chain lengths than the predominant long-chain oleochemicals derived from plants and animals^{7,8,10}. Production of these oleochemicals from cheap feedstocks, like plant biomass, is essential for these bioderived products to compete with their petroleum-derived counterparts. *P. putida* offers considerable advantages over *E. coli* and other more readily engineered microorganisms when it comes to producing oleochemicals from plant-derived feedstocks because of its ability to utilize and valorize lignocellulosic biomass²⁰. The *P. putida* strains engineered in this work provide an important platform to produce FFA derived-oleochemicals from plant-derived feedstocks in this host.

Microbial oleochemical production benefits from the use of a host unable to catabolize fatty acids. Many oleochemical final products or intermediates can be degraded via β -oxidation³⁷, resulting in a decreased ability to accumulate the final product^{27,38}. By removing several CoA ligases that initiate β -oxidation, we engineered *P. putida* strains unable to catabolize medium- and long-chain FFAs. Furthermore, the FFA product profile of several thioesterases was validated in *P. putida*, providing a reference for researchers that aim to produce a variety of FFA profiles in this organism.

The presence of CoA ligase paralogs with overlapping, but different, substrate ranges in *P. putida* is not surprising given its environmental niche as a saprophyte, where it likely encounters a diverse range of fatty acids. In this study, we took advantage of differences in CoA ligase substrate specificity to engineer two strains, $\Delta PP_{0763} \Delta PP_{4549}$ and $\Delta PP_{4549-50}$, that preferentially produce medium- or long-chain FFAs, respectively. This strategy may be leveraged in a variety of microbial hosts to control the final product range of oleochemicals by allowing the catabolism of unwanted FFA-like intermediates and final products. As an example, one could potentially limit the production of unwanted straight-chain FFAs in *E. coli* that have been engineered to produce branched-chain FFAs³⁹ by introducing an engineered CoA ligase that is able to ligate straight-chained FFAs while avoiding the desired branch-chained final products. The overexpression of strategic CoA ligases can be used in conjunction with other chain-length control measures such as engineered thioesterases⁴⁰, acyl-ACP:CoA transacylases³⁸, and engineered fatty acid synthases⁴¹ to further control final product profiles.

Finally, this work provides *P. putida* strains that produce FFA titers of up to 670.9 mg/L total FFAs and 253.6 mg/L C8 FFA. These *P. putida* strains were also grown on sorghum hydrolysate, an industrially relevant plant-derived feedstock with lignocellulosic components that *P. putida* is capable of catabolizing, resulting in the production of medium-chain FFAs at titers greater than 450 mg/L. Additionally, the use of a medium-chain fatty acid methyltransferase demonstrated the utility of strains that could produce FFAs, resulting in a reported FAME titer of 302.4 mg/L. These titers fall below those achieved in *Escherichia*

coli^{25,32,38,40,42,43} and *Yarrowia lipolytica*^{41,44,45}, which indicates there is room for improvement by adopting the engineering strategies used in these classic oleochemical hosts as well as those used in alternative hosts such as *Saccharomyces cerevisiae*⁴⁶ and *Synechocystis* sp. PCC 6803⁴⁷ (Supplementary Tables 8 and 9). One such engineering strategy that has proven to be extremely powerful and led to an impressive FFA titer of 4.7 g/L by Wu et al.⁴² is redox cofactor balancing, which aims to maintain an adequate supply of NADH reducing equivalents that are integral for fatty acid biosynthesis. Similarly, when producing methyl esters, a SAM dependent process, increasing the availability of SAM has led to increased titers^{43,48}. Nevertheless, this work provides a solid framework for *P. putida* metabolic engineers that seek to use this advantageous host to produce oleochemicals from a variety of feedstocks.

Methods

Chemicals. All chemicals were purchased from Sigma-Aldrich (United States) unless otherwise described.

Plasmids and strains. Plasmids and strains used in this study are listed in Supplementary Tables 10, 11. The plasmids and strains have been deposited in the public version of JBEI registry (<http://public-registry.jbei.org>) and are physically available from the corresponding author upon request. All plasmids were constructed via Gibson or Golden Gate Assembly using standard protocols. All heterologous genes were codon optimized for *P. putida* KT2440 and ordered as gBlocks from IDT.

Culture conditions and plasmid transformations. *E. coli* cultures used for cloning were grown in LB medium at 37 °C at 200 RPM, while *P. putida* cultures used for strain construction were grown in LB medium at 30 °C at 200 RPM. Selection markers were used at the following final concentrations: kanamycin (50 μ g/mL), gentamicin (30 μ g/mL), chloramphenicol (20 μ g/mL), and sucrose (20% w/v). Episomal plasmids were transformed into *E. coli* and *P. putida* via electroporation. Briefly, to prepare competent cells 1 mL of overnight culture was centrifuged in 1.7 mL Eppendorf tubes at 21,300 \times g for 1 min. The supernatant was discarded, and pellets were washed with nanopure water three times. After the final wash the pellet was resuspended in 100 μ L of nanopure water and 1 μ L of purified plasmid was added to the competent cells. Cells were electroporated in a 0.1 cm cuvette at 1.8 kV. After electroporation, cells were resuspended in 500 μ L LB and incubated at 37 °C at 200 RPM (*E. coli*) for one hour or 30 °C at 200 RPM (*P. putida*) for two hours before plating. Unless otherwise noted, cultures were grown in 50 mL 25 mm \times 150 mm round-bottom borosilicate culture tubes.

Growth media. For FFA degradation assays EZ Rich medium (Teknova) supplemented with 10 mM glucose was used. For FFA and FAMES production assays either EZ Rich medium supplemented with 100 mM glycerol, Terrific Broth medium (EMD Millipore), or diluted sorghum hydrolysate was used. Sorghum hydrolysate was diluted 4x with M9 minimal salts medium to a final 1x M9 salts concentration. After preparation, all media were sterile filtered, not autoclaved, through a 0.22 μ m bottle-top filter.

Sorghum hydrolysate production. Sorghum (30% w/w of total weight), choline hydroxide (4% w/w of dry sorghum), lactic acid (6.3% of dry sorghum), acetic acid (5.8% of dry sorghum), and water were added to a 10 L Parr reactor with a total working mass of 3 kg. Lactic and acetic acid was added to react with choline hydroxide and produce cholinium lactate and cholinium acetate in situ as the pretreatment catalysts. The material was pretreated for three hours at 140 °C at 80 RPM. Subsequently, the pretreated slurry was cooled to 25 °C and the pH was adjusted to 5.0 with 6 N hydrochloric acid. A 9:1 ratio of cellulase CTec3 and hemicellulase HTec3 NS 22244 at 10 mg protein/g of biomass was added to the Parr reactor and enzymatic saccharification was conducted at 50 °C for 72 h at 80 RPM. After 72 h, the hydrolysate was centrifuged, and the supernatant was filtered through a 0.45 μ m bottle-top filter. Following filtration, the pH of the hydrolysate was adjusted to 7.0 with 5 N NaOH. Finally, the hydrolysate was filtered once more through a 0.22 μ m bottle-top filter. The final hydrolysate contained 47.1 g/L glucose, 25.6 g/L xylose, 16.9 g/L acetic acid, and 17.3 g/L lactic acid.

Generation of CoA ligase knockout mutants. Deletion mutants in *P. putida* were constructed by allelic exchange as described previously⁴⁹. Briefly, 1 kb homology regions upstream and downstream of the target gene, including the start and stop codons, were cloned into pMQ30. Plasmids were then conjugated into *P. putida* using *E. coli* S17 strains. Transconjugants were selected on gentamicin and chloramphenicol LB plates and then grown overnight in LB with no antibiotics. Overnight cultures were diluted 100x, 100 μ L of which was plated on LB agar with

no NaCl that was supplemented with 10% (wt/vol) sucrose. Putative deletions were replica plated on LB agar with no NaCl supplemented with 10% (wt/vol) sucrose and LB agar with gentamicin. Colonies that grew on sucrose, but not gentamicin, were screened via PCR with primers flanking the target gene to confirm gene deletion.

FFA degradation assays. Tested strains were inoculated in 5 mL of EZ Rich medium supplemented with 10 mM glucose and grown overnight at 30 °C and 200 RPM. The cultures and a blank medium-only control were then back diluted 10x in EZ Rich medium supplemented with 10 mM glucose and spiked with 250 μM of each even-chained FFA between C6 and C16. Following this, cultures were grown at 30 °C for 48 h. The remaining FFAs were derivatized and quantified using GC/MS.

Growth assays. Carbon source growth assays were performed as previously described²⁷. Briefly, overnight cultures were inoculated into 5 mL of LB medium from single colonies, and grown at 30 °C. These cultures were washed three times in carbon-free MOPS (morpholinepropanesulfonic acid) minimal medium, which is comprised of 32.5 μM CaCl₂, 0.29 mM K₂SO₄, 1.32 mM K₂HPO₄, 8 μM FeCl₂, 40 mM MOPS, 4 mM tricine, 0.01 mM FeSO₄, 9.52 mM NH₄Cl, 0.52 mM MgCl₂, 50 mM NaCl, 0.03 μM (NH₄)₆Mo₇O₂₄, 4 μM H₃BO₃, 0.3 μM CoCl₂, 0.1 μM CuSO₄, 0.8 μM MnCl₂, and 0.1 μM ZnSO₄. After washing, cultures were diluted 100x into 500 μL of MOPS minimal medium with 10 mM glucose or 10 mM FFA (C6–C12) was spiked in as a sole carbon source in 48-well plates (Falcon, 353072). Tergitol NP-40 was added to the medium to a final concentration of 1% (v/v) to help solubilize the FFAs. Plates were sealed with a gas-permeable microplate adhesive film (Breathe-Easy®, Sigma-Aldrich, Z380059), and then optical density at 600 nm (OD₆₀₀) was monitored with a Biotek Synergy H1M at 30 °C for 48 h with fast continuous shaking (Agilent, Santa Clara, CA). To conduct growth assays on strains containing an IPM overlay, overnight cultures were diluted 100x into 5 mL of LB medium containing a 1:10 isopropyl myristate overlay in 50 mL 25 mm × 150 mm round-bottom borosilicate culture tubes and grown at 30 °C, 200 RPM, for 48 h. Periodically, 100 μL of the culture's aqueous phase was transferred to a clear bottom 96-well plate (VWR, CORN3912) and the OD₆₀₀ was measured with a SpectraMax M2 plate reader.

FFA and FAME production assays. Strains were inoculated in 5 mL of medium containing kanamycin and grown overnight at 30 °C and 200 RPM. The media used for overnight cultures matched the media used for the production assay. Strains grown in sorghum hydrolysate had to be slowly adapted to this medium. First, strains were inoculated in a 20x dilution of hydrolysate in M9 minimal salts medium overnight, and subsequently back diluted into a 4x dilution of hydrolysate in M9 minimal salts and once again grown overnight. The next day, all overnight cultures were back diluted 10x into kanamycin-containing medium and grown at 30 °C for 4 h before adding arabinose to a final concentration of 0.2% v/v. A 1:10 isopropyl myristate overlay was added to FAME-producing cultures at the time of induction. Following induction with arabinose, cultures were grown for an additional 48 h before quantifying FFA and FAME production via GC/MS.

FFA derivatization and quantification via GC/MS. To derivatize FFAs in liquid culture, 300 μL of culture was added to a 1.5 mL screw cap microcentrifuge tube (VWR 16466-064) containing 15 μL of 40% tetrabutylammonium hydroxide. Each sample was spiked with a nonanoic acid internal standard to a final concentration of 250 μM. Then, 600 μL of dichloromethane containing 0.5% 2,3,4,5,6-penta-fluorobenzyl bromide (v/v) was added to each sample. The samples were incubated in an Eppendorf thermomixer at 50 °C and 1400RPM for 20 min. Following incubation, the samples were centrifuged at 21,300×g for 10 min and the organic layer was collected for GC/MS analysis. In parallel, blank medium samples containing 0 μM, 50 μM, 100 μM, 250 μM, 500 μM, or 750 μM mixture of each even-chained FFA between C6 and C16 were similarly spiked with a nonanoic acid internal standard and derivatized in triplicate.

Samples were run on an Agilent 6890 GC and Agilent 5973 MS using a 30 m × 0.250 mm × 0.25 μm HP-5MS column with a helium flow of 1.3 mL/min. The GC was run in splitless mode with a 1 μL sample injection and a constant inlet temperature and transfer line temperature of 250 °C. The oven starting temperature was 80 °C and held for 1 min. Then, the oven temperature was increased at a rate of 10 °C/min until 150 °C. Finally, the temperature was increased at a rate of 20 °C/min until 300 °C and held for 5 min. A solvent delay of 6.80 min was used and the MS was run in scan mode (50.0–350.0 amu). The extracted ion chromatograms at 181 *m/z*, a prominent fragment ion for pentafluorobenzyl esters, were analyzed via Chemstation Enhanced Data Analysis program. We identified compounds of interest by comparison with derivatized authentic standards.

Linear regression was used to generate a standard curve for each derivatized FFA using standards between 0 and 750 μM. More specifically, the extracted ion chromatogram peak area of the FFA of interest was normalized by the extracted ion chromatogram peak area of the derivatized nonanoic acid internal standard within each sample to generate an area ratio for each FFA present in the standard. Similarly, the average area ratios from biological replicates (*n* = 3) were calculated

for each FFA present in the samples and compared to a standard curve generated in the same media to determine the concentration of the FFA. If any calculated FFA area ratio within a sample fell outside the linear range of the standard curve, then a fresh aliquot of the sample was diluted 5x in media, spiked with internal standard, and re-analyzed to more accurately calculate the concentration of the FFA.

FAME quantification via GC/MS. All medium-chain FAMES were found to evaporate from liquid media when maintained at 30 °C and 200RPM for 48 h. Therefore, a 1:10 isopropyl myristate (IPM) overlay was used in all samples from which we quantified FAME titers. Once ready for analysis, 1 mL from the surface of each sample was centrifuged at 21,300×g for 10 min. After centrifugation, 20 μL of the IPM layer was collected and diluted 10x with ethyl acetate spiked with 500 μM methyl nonanoate as an internal standard. In parallel, FAME standards were prepared by creating a 0 μM, 50 μM, 100 μM, 250 μM, 500 μM, 750 μM, 1 mM, 1.5 mM, and 2 mM mixture of each even-chained FAME between C6 and C16 in a 1:10 solution of IPM in ethyl acetate spiked with 500 μM methyl nonanoate as an internal standard in triplicate.

Samples were run on an Agilent 6890 GC and Agilent 5973 MS using a 30 m × 0.250 mm × 0.25 μm HP-5MS column with a helium flow of 1.3 mL/min. The GC was run in splitless mode with a 1 μL sample injection and a constant inlet temperature and transfer line temperature of 280 °C. The oven starting temperature was 50 °C and held for 1 min. Then, the oven temperature was increased at a rate of 10 °C/min until 160 °C. Finally, the temperature was increased at a rate of 30 °C/min until 250 °C and held for 5 min. A solvent delay of 4.8 min was used and the MS was run in scan mode (50.0–350.0 amu). The extracted ion chromatograms at 74 *m/z*, a prominent fragment ion for FAMES, were analyzed via Chemstation Enhanced Data Analysis program. We identified compounds of interest by comparison with authentic standards.

Linear regression was used to generate a standard curve for each FAME using standards between 0 and 2 mM. More specifically, the extracted ion chromatogram peak area of the FAME of interest was normalized by the extracted ion chromatogram peak area of the methyl nonanoate internal standard within each sample to generate an area ratio for each FAME present in the standard. Similarly, the average area ratios from biological replicates (*n* = 3) were calculated for each FAME present in samples and compared to the standard curve to determine the concentration of the FAME.

Despite the use of an IPM overlay, we found that medium-chain FAMES were still partially evaporating. To account for this, every production run had blank media controls (*n* = 3) that were spiked with a 500 μM FAME mixture before the addition of the IPM overlay. These controls were incubated alongside all biological samples and were similarly processed for FAME quantification. The average area ratios of each FAME in the spiked FAME controls were compared to the area ratios corresponding to 500 μM FAME in the standard curves and used to calculate an evaporation coefficient that accounts for the evaporation of FAMES following the formula below (Eq. 1):

$$E = \frac{A_{\text{standard}}}{A_{\text{spiked}}} \quad (1)$$

where A_{standard} is the expected area ratio of a particular 500 μM FAME as calculated from the standard curve and A_{spiked} is the observed area ratio of a particular 500 μM FAME that was spiked into a media control and incubated alongside biological samples. After calculating this coefficient for each FAME, this value was multiplied by the original calculated FAME concentration to determine a FAME concentration adjusted for evaporation.

Theoretical yield calculations. Using the COBRApy metabolic modeling package in Python⁵⁰, the maximum theoretical yield was calculated with the *P. putida* KT2440 model IJN1463⁵¹ assuming no carbon flux to biomass. Individual thioesterase reactions were added for each free fatty acid analyte and methyl transferase reactions for the methyl ester analytes.

Statistics and reproducibility. All experiments involving the quantification of FFAs or FAMES from bacterial liquid cultures were conducted with three biologically independent samples (*n* = 3) where each replicate was started from a different colony. The reported values were the mean of these biologically independent samples and error bars show the standard error of the mean.

Reporting summary. Further information on research design is available in the Nature Portfolio Reporting Summary linked to this article.

Data availability

Plasmids and strains used in this study are listed in Supplementary Tables 10, 11. The plasmids and strains have been deposited in the public version of JBEI registry (<http://public-registry.jbei.org>) from which physical strains can be ordered. Source data for Figs. 2–6 and Supplementary Fig. 3 is found in Supplementary Data 1.

Received: 14 October 2022; Accepted: 2 December 2022;

Published online: 12 December 2022

References

- Rupilius, W. & Ahmad, S. Palm oil and palm kernel oil as raw materials for basic oleochemicals and biodiesel. *Eur. J. Lipid Sci. Technol.* **109**, 433–439 (2007).
- Zhou, Y. J. et al. Production of fatty acid-derived oleochemicals and biofuels by synthetic yeast cell factories. *Nat. Commun.* **7**, 11709 (2016).
- Biermann, U., Bornscheuer, U., Meier, M. A. R., Metzger, J. O. & Schäfer, H. J. Oils and fats as renewable raw materials in chemistry. *Angew. Chem. - Int. Ed.* **50**, 3854–3871 (2011).
- Persson, U. M., Henders, S. & Cederberg, C. A method for calculating a land-use change carbon footprint (LUC-CFP) for agricultural commodities - applications to Brazilian beef and soy, Indonesian palm oil. *Glob. Chang. Biol.* **20**, 3482–3491 (2014).
- Hoekman, S. K., Broch, A., Robbins, C., Cenicerio, E. & Natarajan, M. Review of biodiesel composition, properties, and specifications. *Renew. Sustain. Energy Rev.* **16**, 143–169 (2012).
- Stournas, S., Lois, E. & Serdari, A. Effects of fatty acid derivatives on the ignition quality and cold flow of diesel fuel. *J. Am. Oil Chem. Soc.* **72**, 433–437 (1995).
- Cruz-Morales, P. et al. Biosynthesis of polycyclopropanated high energy biofuels. *Joule* **6**, 1590–1605 (2022).
- Tao, H., Guo, D., Zhang, Y., Deng, Z. & Liu, T. Metabolic engineering of microbes for branched-chain biodiesel production with low-temperature property. *Biotechnol. Biofuels* **8**, 1–11 (2015).
- Sheppard, M. J., Kunjapur, A. M. & Prather, K. L. J. Modular and selective biosynthesis of gasoline-range alkanes. *Metab. Eng.* **33**, 28–40 (2016).
- Zargar, A. et al. Leveraging microbial biosynthetic pathways for the generation of 'drop-in' biofuels. *Curr. Opin. Biotechnol.* **45**, 156–163 (2017).
- Zhang, R. et al. Lignin valorization meets synthetic biology. *Eng. Life Sci.* **19**, 463–470 (2019).
- Nikel, P. I. et al. Reconfiguration of metabolic fluxes in *Pseudomonas putida* as a response to sub-lethal oxidative stress. *ISME J.* **15**, 1751–1766 (2021).
- Ebert, B. E., Kurth, F., Grund, M., Blank, L. M. & Schmid, A. Response of *Pseudomonas putida* KT2440 to increased NADH and ATP demand. *Appl. Environ. Microbiol.* **77**, 6597–6605 (2011).
- Nikel, P. I. & de Lorenzo, V. *Pseudomonas putida* as a functional chassis for industrial biocatalysis: From native biochemistry to trans-metabolism. *Metab. Eng.* **50**, 142–155 (2018).
- Gauttam, R., Mukhopadhyay, A. & Singer, S. W. Construction of a novel dual-inducible duet-expression system for gene (over)expression in *Pseudomonas putida*. *Plasmid* **110**, 102514 (2020).
- Thompson, M. G. et al. Identification, characterization, and application of a highly sensitive lactam biosensor from *Pseudomonas putida*. *ACS Synth. Biol.* **9**, 53–62 (2020).
- Loeschcke, A. & Thies, S. Engineering of natural product biosynthesis in *Pseudomonas putida*. *Curr. Opin. Biotechnol.* **65**, 213–224 (2020).
- Eng, T. et al. Engineering *Pseudomonas putida* for efficient aromatic conversion to bioproduct using high throughput screening in a bioreactor. *Metab. Eng.* **66**, 229–238 (2021).
- Lim, H. G. et al. Generation of *Pseudomonas putida* KT2440 strains with efficient utilization of xylose and galactose via adaptive laboratory evolution. *ACS Sustain. Chem. Eng.* **9**, 11512–11523 (2021).
- Lim, H. G. et al. Generation of ionic liquid tolerant *Pseudomonas putida* KT2440 strains via adaptive laboratory evolution. *Green Chem.* **22**, 5677–5690 (2020).
- Wang, W., Xu, P. & Tang, H. Sustainable production of valuable compound 3-succinoyl-pyridine by genetically engineering *Pseudomonas putida* using the tobacco waste. *Sci. Rep.* **5**, 1–11 (2015).
- Bentley, G. J. et al. Engineering glucose metabolism for enhanced muconic acid production in *Pseudomonas putida* KT2440. *Metab. Eng.* **59**, 64–75 (2020).
- Sarwar, A., Nguyen, L. T. & Lee, E. Y. Bio-upgrading of ethanol to fatty acid ethyl esters by metabolic engineering of *Pseudomonas putida* KT2440. *Bioresour. Technol.* **350**, 126899 (2022).
- Lennen, R. M. & Pfleger, B. F. Engineering *Escherichia coli* to synthesize free fatty acids. *Trends Biotechnol.* **30**, 659–667 (2012).
- Hernández Lozada, N. J. et al. Highly active C 8 -acyl-ACP thioesterase variant isolated by a synthetic selection strategy. *ACS Synth. Biol.* **7**, 2205–2215 (2018).
- Morgan-Kiss, R. M. & Cronan, J. E. The *Escherichia coli* fadK (ydiD) gene encodes an anaerobically regulated short chain acyl-CoA synthetase. *J. Biol. Chem.* **279**, 37324–37333 (2004).
- Thompson, M. G. et al. Fatty acid and alcohol metabolism in *Pseudomonas putida*: functional analysis using random barcode transposon sequencing. *Appl. Environ. Microbiol.* **86**, e01665–20 (2020).
- Cho, H. & Cronan, J. E. Defective export of a periplasmic enzyme disrupts regulation of fatty acid synthesis. *J. Biol. Chem.* **270**, 4216–4219 (1995).
- Bi, C. et al. Development of a broad-host synthetic biology toolbox for *Ralstonia eutropha* and its application to engineering hydrocarbon biofuel production. *Microb. Cell Fact.* **12**, 1–10 (2013).
- Massey, L. K., Conrad, R. S. & Sokatch, J. R. Regulation of leucine catabolism in *Pseudomonas putida*. *J. Bacteriol.* **118**, 112–120 (1974).
- Petronikolou, N. & Nair, S. K. Biochemical studies of mycobacterial fatty acid methyltransferase: a catalyst for the enzymatic production of biodiesel. *Chem. Biol.* **22**, 1480–1490 (2015).
- Nawabi, P., Bauer, S., Kyrpides, N. & Lykidis, A. Engineering *Escherichia coli* for biodiesel production utilizing a bacterial fatty acid methyltransferase. *Appl. Environ. Microbiol.* **77**, 8052–8061 (2011).
- Elmore, J. R., Furches, A., Wolff, G. N., Gorday, K. & Guss, A. M. Development of a high efficiency integration system and promoter library for rapid modification of *Pseudomonas putida* KT2440. *Metab. Eng. Commun.* **5**, 1–8 (2017).
- Kadisich, M., Schmid, A. & Bühler, B. Hydrolase BioH knockout in *E. coli* enables efficient fatty acid methyl ester bioprocessing. *J. Ind. Microbiol. Biotechnol.* **44**, 339–351 (2017).
- Tian, Y. et al. Overexpression of the rice BAHD acyltransferase AT10 increases xylan-bound p-coumarate and reduces lignin in *Sorghum bicolor*. *Biotechnol. Biofuels* **14**, 1–9 (2021).
- Dong, J. et al. Methyl ketone production by *Pseudomonas putida* is enhanced by plant-derived amino acids. *Biotechnol. Bioeng.* **116**, 1909–1922 (2019).
- Kassab, E., Fuchs, M., Haack, M., Mehlmer, N. & Brueck, T. B. Engineering *Escherichia coli* FAB system using synthetic plant genes for the production of long chain fatty acids. *Microb. Cell Fact.* **18**, 1–10 (2019).
- Yan, Q. et al. Metabolic engineering strategies to produce medium-chain oleochemicals via acyl-ACP:CoA transacylase activity. *Nat. Commun.* **13**, 1619 (2022).
- Haushalter, R. W. et al. Production of anteiso-branched fatty acids in *Escherichia coli*; next generation biofuels with improved cold-flow properties. *Metab. Eng.* **26**, 111–118 (2014).
- Grisewood, M. J. et al. Computational redesign of Acyl-ACP thioesterase with improved selectivity toward medium-chain-length fatty acids. *ACS Catal.* **7**, 3837–3849 (2017).
- Wang, K. et al. Engineering *Yarrowia lipolytica* to produce tailored chain-length fatty acids and their derivatives. *ACS Synth. Biol.* **11**, 2564–2577 (2022).
- Wu, J. et al. Improving metabolic efficiency of the reverse beta-oxidation cycle by balancing redox cofactor requirement. *Metab. Eng.* **44**, 313–324 (2017).
- Sherkhanov, S., Korman, T. P., Clarke, S. G. & Bowie, J. U. Production of FAME biodiesel in *E. coli* by direct methylation with an insect enzyme. *Sci. Rep.* **6**, 1–10 (2016).
- Xu, P., Qiao, K., Ahn, W. S. & Stephanopoulos, G. Engineering *Yarrowia lipolytica* as a platform for synthesis of drop-in transportation fuels and oleochemicals. *Proc. Natl Acad. Sci. USA* **113**, 10848–10853 (2016).
- Rigouin, C. et al. Production of medium chain fatty acids by *Yarrowia lipolytica*: combining molecular design and TALEN to engineer the fatty acid synthase. *ACS Synth. Biol.* **6**, 1870–1879 (2017).
- Gajewski, J., Pavlovic, R., Fischer, M., Boles, E. & Grininger, M. Engineering fungal de novo fatty acid synthesis for short chain fatty acid production. *Nat. Commun.* **8**, 14650 (2017).
- Yunus, I. S., Palma, A., Trudeau, D. L., Tawfik, D. S. & Jones, P. R. Methanol-free biosynthesis of fatty acid methyl ester (FAME) in *Synechocystis* sp. PCC 6803. *Metab. Eng.* **57**, 217–227 (2020).
- Luo, Z. W., Cho, J. S. & Lee, S. Y. Microbial production of methyl anthranilate, a grape flavor compound. *Proc. Natl Acad. Sci. USA* **166**, 10749–10756 (2019).
- Thompson, M. G. et al. Omics-driven identification and elimination of valerolactam catabolism in *Pseudomonas putida* KT2440 for increased product titer. *Metab. Eng. Commun.* **9**, e00098 (2019).
- Ebrahim, A., Lerman, J. A., Palsson, B. O. & Hyduke, D. R. COBRAPy: COntstraints-based reconstruction and analysis for python. *BMC Syst. Biol.* **7**, 74 (2013).
- King, Z. A. et al. BiGG Models: a platform for integrating, standardizing and sharing genome-scale models. *Nucleic Acids Res.* **44**, D515–D522 (2016).
- Choi, Y. J. & Lee, S. Y. Microbial production of short-chain alkanes. *Nature* **502**, 571–574 (2013).
- Deng, X. et al. Structure-guided reshaping of the acyl binding pocket of *TesA* thioesterase enhances octanoic acid production in *E. coli*. *Metab. Eng.* **61**, 24–32 (2020).

Acknowledgements

We thank Chris Eiben for his advice on analytical chemistry, Ellen Zippi for her guidance on the manuscript, and Yuzhong Liu & Amin Zargar for valuable discussions. This work

was part of the DOE Joint BioEnergy Institute (<https://www.jbei.org>) supported by the U.S. Department of Energy, Office of Science, Office of Biological, and Environmental Research, and supported by the U.S. Department of Energy, Energy Efficiency and Renewable Energy, Bioenergy Technologies Office, through contract DE-AC02-05CH11231 between Lawrence Berkeley National Laboratory and the U.S. Department of Energy. L.E.V. was supported by a National Science Foundation Graduate Research Fellowship, M.G.T. is a Simons Foundation Awardee of the Life Sciences Research Foundation, and M.M. was supported by the Amgen Scholars program. The laboratory of L.M.B. is partially funded by the Deutsche Forschungsgemeinschaft (DFG, German Research Foundation) under Germany's Excellence Strategy within the Cluster of Excellence FSC 2186 "The Fuel Science Center."

Author contributions

Conceptualization: L.E.V., M.R.I., and J.D.K.; methodology: L.E.V., M.R.I., M.S., A.N.P., N.S., A.O., J.G., and J.D.K.; investigation: L.E.V., M.R.I., M.S., A.N.P., M.G.T., J.R., M.M., K.Y., N.S., and A.O.; writing – original draft: L.E.V.; writing – review and editing: all authors; resources and supervision: P.M.S., L.M.B., J.G., and J.D.K.

Competing interests

J.D.K. has financial interests in Amyris, Ansa Biotechnologies, Apertor Pharma, Berkeley Yeast, Demetrix, Lygos, Napigen, ResVita Bio, Zero Acre Farms, and Cyklos Materials. The other authors declare no competing interests.

Additional information

Supplementary information The online version contains supplementary material available at <https://doi.org/10.1038/s42003-022-04336-2>.

Correspondence and requests for materials should be addressed to Jay D. Keasling.

Peer review information *Communications Biology* thanks the anonymous reviewers for their contribution to the peer review of this work. Primary Handling Editor: George Inglis. Peer reviewer reports are available.

Reprints and permission information is available at <http://www.nature.com/reprints>

Publisher's note Springer Nature remains neutral with regard to jurisdictional claims in published maps and institutional affiliations.



Open Access This article is licensed under a Creative Commons Attribution 4.0 International License, which permits use, sharing, adaptation, distribution and reproduction in any medium or format, as long as you give appropriate credit to the original author(s) and the source, provide a link to the Creative Commons license, and indicate if changes were made. The images or other third party material in this article are included in the article's Creative Commons license, unless indicated otherwise in a credit line to the material. If material is not included in the article's Creative Commons license and your intended use is not permitted by statutory regulation or exceeds the permitted use, you will need to obtain permission directly from the copyright holder. To view a copy of this license, visit <http://creativecommons.org/licenses/by/4.0/>.

© The Author(s) 2022